Effects of Fault Displacement on Earth Structures above Active Fault

Yasuyuki Nabeshima

National Institute of Technology, Akashi College, Akashi, Japan
Email: nabesima@akashi.ac.jp

***Abstract*—The concern for the collapse of structures by active fault displacement has increased since the 1999 Taiwan Chi-Chi earthquake and the 2016 Kumamoto earthquake. Many infrastructures in Japan, such as bridges, earth dams and embankments, have not been designed considering the fault displacements. In this paper, the effect of fault displacement on earth structures above the active fault was discussed through a series of model tests where aluminum rod models were used as the ground. Consequently, the shear bands developed from the bottom to the ground surface regardless of the ground thickness and the type of active faults. The deformation of the ground surface due to the fault displacement was not limited within the area above the active fault. As the ground became thicker, the area of the surface deformation expanded wider.**

***Keywords*—fault displacement, earth structure, active fault, earthquake, model test**

I. Introduction

The fault displacement caused major damage to the 23-meter-high Oohata dam (an agricultural dam) above the Futagawa fault in the 2016 Kumamoto earthquake, as shown in Fig. 1. Fortunately, the Oohata dam did not collapse, but a large amount of water was leaked from the dam, and evacuation orders were issued for the hazardous area of the dam collapse. Also, the Oohata Bridge on the Kumamoto prefectural route 28 in the same area was sever damaged by the fault deformation [1–3].

Fig. 1. Damage of the Oohata dam due to the fault displacement.

The 2011 Tohoku earthquake also caused the collapse of main embankment of the Fujinuma dam and cause a sever debris flow to the downstream area and 7 people were dead [4]. In overseas cases, the 1999 Chi-Chi earthquake that occurred in Taiwan brought fault lines to the surface in the cities of Nantou and Taichung prefectures and caused catastrophic damage to buildings and structures directly above and around the faults due to the fault displacement. As a representative example, at the gravity concrete dam as shown in Fig. 2, the fault displacement uplifted the riverbed and caused a nearly 10-meter gap between the riverbed and the dam. The intake weir collapsed due to the fault displacement. After the Chi-Chi earthquake, the design and the countermeasures should be taken into the consideration for infrastructures in case of faults appear on the ground surface and large fault displacement occurs [5–8].

Fig. 2. Damage of the gravity concrete dam in the 1999 Chi-Chi earthquake (panel of the 921 Earthquake Museum of Taiwan).

Thus, important infrastructures which were located above the active fault are necessary to consider the ground surface displacement due to the fault displacement. The model ground by using aluminum rods instead of real soil was adopted to quantitatively evaluate the amount of ground surface deformation associated with the fault displacement. The effect of the fault displacement on damage of the earth structure above active fault was discussed.

II. Damage of Structures Above Active Fault Due to Fault Displacement

A. The 1999 Taiwan Chi-Chi Earthquake

The 1999 Taiwan Chi-Chi earthquake, which occurred at 1:47 a.m. on September 21, 1999, had a magnitude of

Manuscript received November 11, 2023; revised December 21, 2023; accepted January 4, 2024; published July 20, 2024.

7.3 on the Richter scale and an epicenter near Chi-Chi, Nantou prefecture, with an estimated depth of 6.99 km [5]. The tremor was felt throughout Taiwan, with intensity levels of 6 recorded in Wufeng District, Taichung in central Taiwan [5]. The earthquake occurred along the Chelungpu Fault in the western part of the island of Taiwan. The fault stretches along the foothills of the central mountains in Nantou and Taichung counties. Near the northern end of the fault, a nearly 7 m high waterfall was created by the earthquake as the surface rupture offset the channel of the Dajia river [5]. The total surface rupture was about 100 km in length [6]. Damage caused by the earthquake included 2,415 deaths, 29 missing, 11,305 severely wounded, with 51,711 buildings completely destroyed, 53,768 buildings severely damaged [7, 8]. 102 major bridges were badly damaged, with many having to be torn down [5, 6]. The central cross-island highway, at the time the only major complete route across the mountains in central Taiwan, was badly damaged. There were 132 landslides during the main earthquake and the aftershocks [7, 8].

The major damage of the 1999 Chi-Chi earthquake was reserved in the 921 Earthquake Museum of Taiwan. with the damage remaining as it was. Fig. 3 shows that the ground was uplifted at the Wufeng Township General Sports Ground. The Guangfu Junior High School, located near the sports field and directly above the fault line, was completely destroyed as shown in Fig. 4, and houses in the neighborhood were also damaged. The road and levee on the south side of the playground were also displaced. The fault deformation of the ground surface was 18 to 20 meters at the playground and about 15 meters near the school. The Shigang Dam in Taichung as shown in Fig. 2 was breached by an earthquake fault. Although this site is located far from the epicenter, the fault changed its direction from north-south to east-west in this area, releasing a large amount of energy and causing extensive damage. The vertical displacement of the dam was 9.8 m and it was the highest on the fault. Fig. 5 shows the collapse of the bridge, which is a simple reinforced concrete bridge with a multiple-diameter span located downstream of the Shigang Dam. The fault runs along the left bank of the bridge, and a waterfall appeared in the riverbed area about 10 m upstream due to the fault displacement [9].

Fig. 3. Deformation of sports field due to fault deformation.

Fig. 4. Collapse of the Guangfu Junior High School building.

Fig. 5. Collapse of the bridge and waterfall due to the fault displacement (panel of the 921 Earthquake Museum of Taiwan).

B. The 2016 Kumamoto Earthquake

In the 2016 Kumamoto earthquake, a seismic intensity 7 was observed in Mashiki town at 21:26 on April 14, and two days later, a seismic intensity 7, in which the moment magnitude scale was recorded as 7.0, was observed in Mashiki town and Nishihara village at 1:25 on April 16. Seven earthquakes of seismic intensity 6 or higher occurred between April 14 and 16. The Kumamoto earthquake occurred in a part of the Futagawa and Hinagu fault zones distributed in Kumamoto prefecture as shown in Figs. 6 and 7. The earthquake occurred in the northeastern part of the Futagawa fault zone and Hinagu fault. In the earthquake, about 2 m right-lateral displacement was appeared on the ground surface along with 31 km long.

Fig. 6. Fault deformation in Mashiki town.

Fig. 7. Ground surface above the fault.

III. Methotorogy of Model Tests

A. Model Test Apparatus

In this study, a series of model tests were carried out to investigate the ground deformation above the active fault under the plane-strain condition by using aluminum bar laminates and model soil ground. The two-dimensional model test was carried out because the principal strain in the longest dimension is constrained as effectively zero strain condition. Thus, allowing the two-dimensional analysis of deformation, a cross section of the ground is investigated in this research.

The deformation on the ground surface and under the ground due to the fault displacement was investigated using model tests. In the model tests, a model ground is made from aluminum bar laminates and silica sand. Fault displacement was generated by lifting a base plate, and the deformation of the ground surface and under the ground was investigated. The vertical fault movement and the reverse fault movement were carried out. The vertical fault means that the displacement of the stratum is moved to the vertical direction, while the reverse fault means that the upper plate is lifted and is often found in areas where compressive forces are applied from both sides.

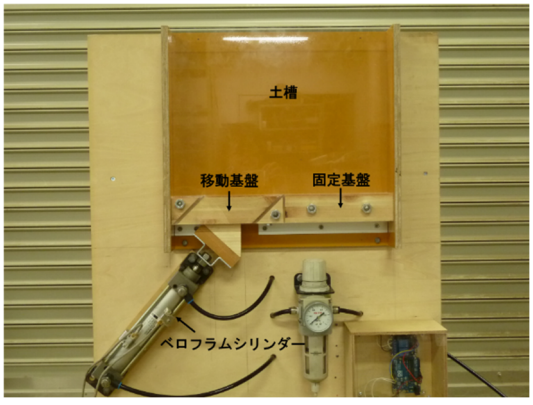

Fig. 8. Model test apparatus simulating fault deformation.

The model test apparatus for simulating the fault deformation has square model box, 400 mm in length, 400 mm in width and 50 mm in depth. Fig. 8 shows the model test apparatus. An acrylic plate was installed in the front of the box to observe the displacement of the aluminum bar laminate and/or the model ground. By changing the orientation of the base and the bellofram cylinder, the apparatus can simulate two types of displacement: vertical fault displacement and the reverse fault displacement at an inclination angle of 45° as shown in Fig. 8. The bellofram cylinder was controlled by air pressure and moved approximately 2 seconds to 25 mm in vertically and 25 mm in diagonally.

B. Aluminum Model Ground

An aluminum rod laminate is a reproduction of the ground using aluminum rods. The aluminum rod laminate does not need to be supported by walls on the front and rear surfaces, so there is no friction between the model ground and the wall. It is also possible to take photographs of the aluminum rod laminate from the front surface, and the displacement and deformation of the ground can be determined by comparing the photographs before and after the experiment [10]. Fig. 9 shows the aluminum model ground in model test apparatus. Two types of aluminum rods, 3 and 5 mm in diameter with 50 mm in length, were used in the aluminum laminate mixing with a weight ratio of 3:2. This weight ratio was chosen because the grain size curve of the aluminum rods was parallel to that of the Toyoura sand [11]. The aluminum model ground has been used to simulate failure mechanism of sliding failure of the soil slope, therefore, the aluminum model ground shows high reliability [12].

Fig. 9. Aluminum model ground in model test apparatus.

The aluminum rods were stacked until their heights reached 100 mm or 150 mm. The 25 mm square grid lines were drawn to observe the aluminum rod movement as shown in Fig. 9. The aluminum rod laminate with 100 mm or 150 mm in height was subjected to the vertical and the reverse fault displacement, and the deformation of the ground surface and under the ground was observed. Two photographs were taken before and after the fault displacement and compared each other.

C. Sand Model Ground

Fig. 10 shows the s and model ground in model test apparatus. A model test was conducted on vertical faults with 100 mm in thickness, because the total weight of wet sand was heavier than the lift capacity of the bellofram cylinder. A model sand ground was prepared by compacting silica sand, adjusted to a moisture content of 5% with the wet density of 1.5 g/cm^3. In the model sand

ground, black color sand was used to make horizontal lines every 25 mm intervals. After the model sand ground was made, the model road embankment with 50 mm in high was made on the model ground surface as shown in Fig. 10. Two photographs were taken before and after the experiment, and the displacement of the ground surface and the deformation in the model ground was observed by using horizontal lines of the black color sand.

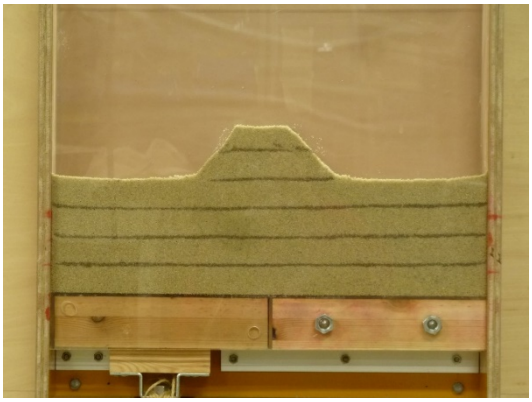

Fig. 10. Sand model ground in model test apparatus.

IV. Result and Discussion

The ground surface displacement and the subsurface deformation of ground were investigated through a series of model tests. The results of the model tests were shown and discussed.

A. Aluminum Model tests with Vertical Displacement

Fig. 11 shows the shallow aluminum model ground deformation after the vertical fault moved. The model ground has 100 mm in thickness. The ground surface of the aluminum model ground showed a large movement above the fault. As shown in Fig. 11, the 25 mm square red grids sheared and deformed above the vertical fault. The deformation area developed from bottom of the fault to the ground surface. Focusing on the aluminum rods near the fault, it could be observed that the ground near the fault loosened after the fault displacement occurred. The 25 mm square red grids did not change except near the fault, therefore, the deformation area concentrated only above the fault. Fig. 12 shows the vector diagram of the lattice points of the red grids in the shallow aluminum model ground. From this figure, the lattice points in the right zone from the fault did not change at all. Vectors above the fault slightly changed to right side.

Fig. 13 shows the vector diagram of the lattice points of the red grids in the thick aluminum model ground. In this case, the thickness of the model ground was 150 mm. This figure also showed the lattice points in the right zone from the fault did not change at all. Vectors above the fault clearly changed to right side through comparison between Figs. 12 and 13. Also, vectors near the left side ground surface above the fault changed to the right side. The deformation area of the ground surface became wider in the thick aluminum model ground. Therefore, the thickness above the fault affected the deformation area on the ground surface. The gap of the ground surface above the fault in the thick model ground was smaller and smoother than that in the shallow model ground.

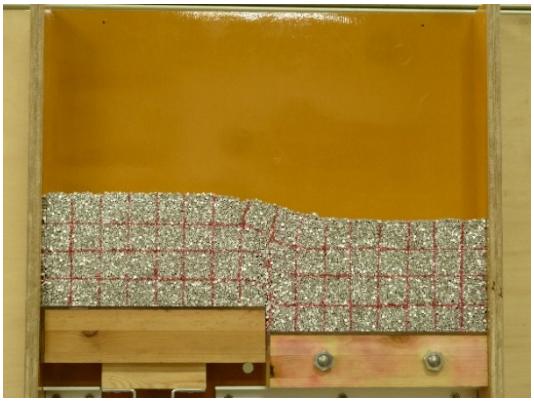

Fig. 11. Shallow aluminum model ground deformation after the vertical fault moved.

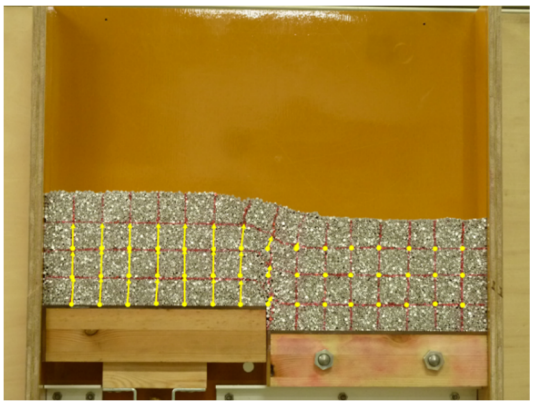

Fig. 12. Vector diagram of the shallow aluminum model ground.

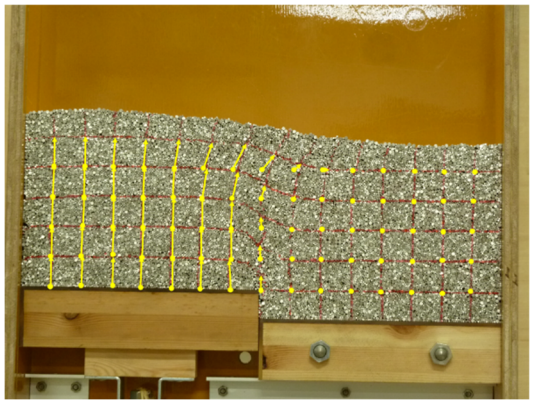

Fig. 13. Vector diagram of thick aluminum model ground.

B. Aluminum Model Tests with Thrust Fault Displacement

Fig. 14 showed the aluminum model ground before the reverse fault moved. The model ground also has 100 mm in thickness. The 25 mm square grids were also drawn on the aluminum rod surface. Fig. 15 showed the aluminum model ground after the reverse fault moved. The base of the apparatus lifted to right above which angle was 45°. The ground surface in Fig. 15 showed asymmetry, because the reverse fault lifted to the right above. Thus, the right side from the center of the reverse fault was discussed to compare the deformation of the model ground, the gray

hatched area in the left side in Figs. 14 and/or 15 was neglected in this paper.

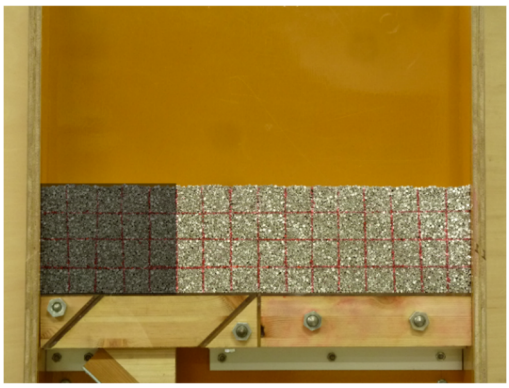

Fig. 14. Aluminum model ground before the reverse fault deformation.

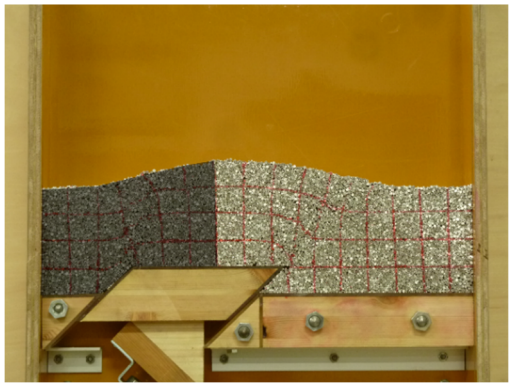

Fig. 15. Aluminum model ground after the reverse fault deformation.

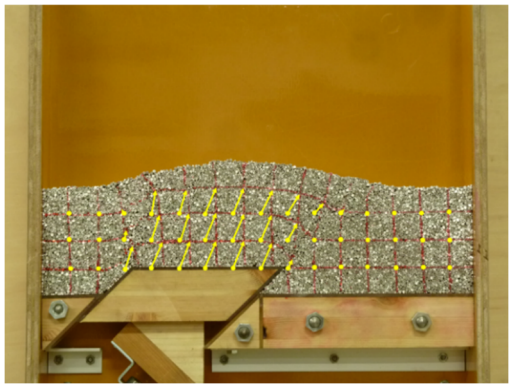

Fig. 16. Vector diagram of shallow aluminum model ground above the reverse fault.

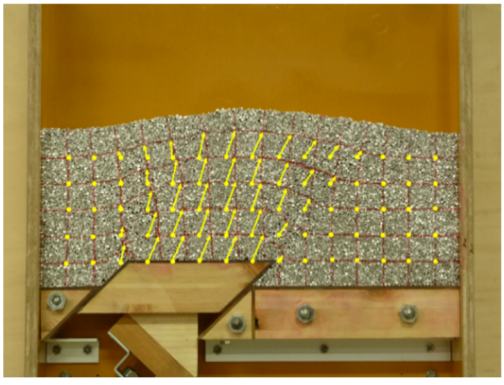

Fig. 17. Vector diagram of thick aluminum model ground above the reverse fault.

While the ground surface concentrated only above the fault in case of the vertical fault, the ground surface in the right side was deformed widely according to the reverse fault movement as shown in Fig. 15. The ground surface deformation in the reverse fault was quite different from that in the vertical fault through the comparison between Figs. 11 and 15. Fig. 16 shows the vector diagram of the lattice points of the red grids in the aluminum model ground with 100 mm thickness in case of the reverse fault. Shear line was not clearly observed and bent from the edge of the reverse fault to the ground surface. Fig. 17 shows the vector diagram in the thick aluminum model ground. In this case, the ground surface above the fault in the thick model ground was small and smooth deformation.

C. Sand Model Test with Vertical Displacement

Fig. 18 showed the deformation of the sand model ground above the vertical fault. Judging from this figure, two shear lines can be observed, one extended straight up from the edge of the fault and the other extended obliquely to the ground surface. They were main fault and a fault diverged from main fault. The diverged shear line extended to the right bottom of the embankment. In the sand model ground, the shear lines appeared very linearly. The gap with 5 mm could be observed at the center of the embankment as the fault displacement due to the reverse fault deformation. Along with the main fault in the center and the diverged fault to right side, a small fault could also be observed at the left bottom of the embankment. The damage of the right side in the embankment was larger than that of the left side. Similar deformation could be observed in the past earthquake damages as shown in Figs. 1 to 3. The damage above the fault could be simulated in the sand model ground. The seismic damage of the embankment was very severe, therefore, countermeasures should be considered to account for the interaction between the fault and earth structures such as embankment [13], and the practical procedure of the highway bridge considering the effect of the active fault deformation was proposed [14]. The surface displacement due to the active fault was one of the most important factors to decide the countermeasures.

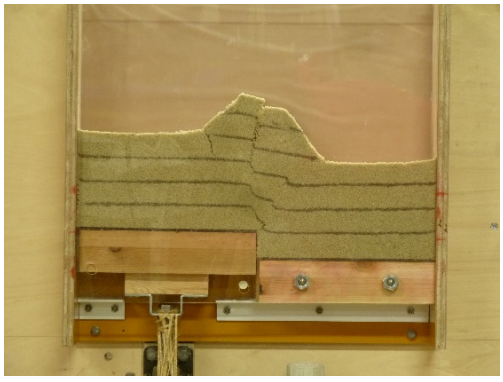

Fig. 18. Deformation of the sand model ground above the vertical fault.

V. Conclusion

The author carried out a series of experimental model tests by using aluminum rod ground to consider the

deformation of the ground above the active fault. The main conclusions in this study were summarized as follows:

(1) The deformation area concentrated only above the fault in case of the vertical fault.
(2) While the ground surface concentrated only above the fault in case of the vertical fault, the ground surface in case of the reverse fault was deformed widely according to the reverse fault movement.
(3) The thickness above the fault affected the deformation area on the ground surface. The gap of the ground surface above the fault in the thick model ground was smaller and smoother than that in the shallow model ground.
(4) The damage above the fault was simulated in the sand model ground. The shear lines appeared very linearly in the sand model ground. The gap was observed at the center of the embankment as the fault displacement.

This experimental research was very fundamental to understand the effect of the active fault on the earth structures. Further experiments of the active fault deformation are necessary to recommend practical suggestions.

The motivation of this study was the survey of damage in the 1999 Kumamoto earthquake. The damage to structures above the active fault was very severe in the earthquake. The Japanese seismic design of infrastructures was designed against strong seismic motion, but that the seismic design due to the large ground displacement or deformation has not been considered. Therefore, the author started this study as a first step.

Conflict of Interest

The author declares no conflict of interest.

Acknowledgment

The authors wish to thank Ms. Yuno Sanda. She was a student in Akashi College and her experimental works were very helpful in this study. Major part of experimental result in this paper was based on her thesis.

References

[1] Y. Hisada, S. Tanaka, J. Kaneda, A. Teramoto, W. Nakamura, M. Murakami, Y. Masuzawa, S. Sakai, K. Nakano, K. Mori, and K. Kimoto, "Investigation of building damage near surface fault rupture of the 2016 Kumamoto Earthquake and countermeasures for active faults," *Journal of Japan Association for Earthquake Engineering*, vol. 20, no. 2, pp. 90–132, 2020. (in Japanese)
[2] Y. Miyazaki, "Landslide disaster triggered by the 2016 Kumamoto Earthquake in and around Minamiaso village, western part of Aso caldera, southwestern Japan," *Journal of Geography*, vol. 125, no. 3, pp. 421–429, 2016. (in Japanese)
[3] T. Hashimoto, T. Tobita, and K. Ueda, "The report of the damage by Kumamoto Earthquake in Maski-machi, Hishihara-mura and Minamiaso-mura," *Anuals of DPRI*, Kyoto University, No. 59B, pp. 125–134, 2016. (in Japanese)
[4] N. Tabuchi, "The break down of Fujinuma dam and the safety of the people," *Journal of Water and Environmental Issues*, vol. 28, no. 2, pp. 159–164, 2015. (in Japanese)
[5] J. C. Lee, H. T. Chu, J. Angelier, Y. C. Chan, J. C. Hu, C. Y. Lu, and R. J. Rau, "Geometry and structure of northern surface ruptures of the 1999 Mw=7.6 Chi-Chi Taiwan earthquake: Influence from inherited fold belt structures," *Journal of Structural Geology*, vol. 24, no. 1, pp. 173–192, 2002.
[6] A. Lin, T. Ouchi, A. Chen, and T. Marayuma, "Co-seismic displacements, folding and shortening structures along the Chelungpu surface rupture zone occurred during the 1999 Chi-Chi (Taiwan) earthquake," *Tectonophysics*, vol. 330, no. (3–4), pp. 225–244, 2001.
[7] T. Iwatate and M. Yoshimine, "Damage characteristics of civil engineering structures by the 1999 Ji-Ji Earthquake, Taiwan," *Comprehensive Urban Studies*, no. 72, pp. 77–115, 2000. (in Japanese)
[8] A. Nakasuji, M. Taniuchi. M. Sano, S. Tsukamoto, and K. Fujiwara, "Outline of damage caused by large Taiwan earthquake (Chi-Chi Earthquake) on Sep. 1999," *Journal of the Japan Society of Engineering Geology*, vol. 41, no. 3, pp. 155–164, 2000. (in Japanese)
[9] M. L. Lin, C. H. Lin, C. H. Li, C. Y. Liu, and C. H. Hung, "3D modeling of the ground deformation along the fault rupture and its impact on engineering structures: Insights from the 1999 Chi-Chi earthquake, Shigang District, Taiwan," *Engineering Geology*, vol. 281, no. 105993, 2021.
[10] Y. Isobe, H. M. Shahin, T. Nakai, R. Sakai, and Y. S. Yoshida, "Restraint effect of ground displacement by sheet pile," *Journal of Geotechnical Engineering*, vol. 10, no. 1, pp. 141–155, 2015. (in Japanese)
[11] N. Onizuka, S. Iitake, and T. Kanai, "Small model test of vertical fault on stack of aluminum rods," *Annual Research Report in Kisarazu Kosen*, vol. 30, pp. 15–18, 1997. (in Japanese)
[12] T. Tsuchikura, "Experiment and simulation of sliding failure using stacks of aluminum rods," in *Proc. 38th Japan Geotechnical Society annual conference*, 2003, pp. 453–454. (in Japanese)
[13] K. Tokida, "Engineering viewpoints on countermeasures for civil engineering structures against surface faulting," *Journal of JSCE*, no. 752, I-66, pp. 63–77, 2004. (in Japanese)
[14] K. Tokida, T. Watanabe, and H. Hiraishi, "Countermeasures for a highway bridge against an active surface fault displacement," in *Proc. 28th JSCE Earthquake Engineering Symposium*, pp. 1–10, 2005. (in Japanese)